euspen's 23rd International Conference & Exhibition, Copenhagen, DK, June 2023
www.euspen.eu

Image-processing-based analysis of subsurface damage in diamond wire sawing of silicon wafer

Chi Fai Cheung*, Huapan Xiao, Chunjin Wang

State Key Laboratory of Ultra-precision Machining Technology, Department of Industrial and Systems Engineering, The Hong Kong Polytechnic University, Hung Hom, Kowloon, Hong Kong, China

**Benny.Cheung@polyu.edu.hk*

Abstract

Subsurface damages (SSDs) greatly deteriorate the mechanical properties and increase the processing costs of the wire-sawn silicon wafer, which should be evaluated accurately and quickly. In this paper, a theoretical model is presented for determining the SSD depth with the surface fracture parameters of the silicon wafer based on the scratch fracture mechanics of brittle materials. Meanwhile, an image processing method is integrated into the model to extract the fracture parameters. To validate the model, a series of experiments were carried out on (100) single-crystal silicon ingots using multi-wire sawing equipment under various slicing parameters. The wafer surface morphology was observed by laser scanning confocal microscopy, and its subsurface morphology was determined by cross-section scanning microscopy. The determined SSD depth is compared with the experimental one. The result shows that the image-processing-based model can accurately and quickly determine the SSD depth in the silicon wafer with an average relative error of less than 12% and within about 15 seconds. The model provides an important means for non-invasive evaluation of the SSDs in diamond wire sawing of silicon wafer.

Subsurface damage, Diamond wire sawing, Silicon Wafer, Image processing

1. Introduction

Due to its excellent semiconductor performance, the silicon wafer is widely used in integrated circuits and photovoltaic industries. The diamond wire sawing is the first procedure for processing the silicon wafer where the SSDs mainly in the form of microcracks are generated inevitably [1]. The SSDs reduce the wafer fracture strength and increase its fragment rate. The SSDs need to be relieved by subsequent grinding and polishing, thus reducing the processing efficiency and increasing the manufacturing cost [2]. As a result, it is very important to evaluate the SSDs in the wire-sawn silicon wafer.

The experimental evaluation of SSDs has been studied which focuses on the changing of SSDs with processing parameters and abrasive geometries. For example, Costa et al. [3] reported that the microcrack depth increased when both feed rate and wire tension increased, while it decreased when wire speed increased. Teomete [4] discovered that the SSD depth was unchanged when the feed rate increased proportionally to the wire speed. Suzuki et al. [5] revealed that an increasing abrasive grit size led to more microcracks. Kumar et al. [6] demonstrated that the subsurface crack became deep slightly when the abrasive wear increased. The experimental evaluation is time-consuming and expensive, and the involved formation mechanism of SSDs is not revealed. For this reason, the theoretical evaluation of SSDs has been investigated which emphasizes the modeling of SSD depth.

For example, based on the indentation fracture mechanics of brittle materials, Liu et al. [7] correlated the SSD depth with the maximum extended length of the median crack, which had a maximum error of 11.6%. Based on the scratch fracture mechanics, Xiao et al. [8] developed a SSD depth model with a maximum error of less than 15.0%. Wang et al. [9] built a model to determine the subsurface crack depth using the half-penny crack system rather than the median-lateral crack system, which had the maximum error of 5.8%. These SSD depth models have achieved a small error, but their establishment process is very hard, which involves the modeling of material properties, saw wire, scratch groove, etc. This is tedious and inconvenient, and greatly depends on professional knowledge. Consequently, a simpler model or a quicker method needs to be proposed.

Based on the scratch fracture mechanics, the SSD depth is modelled with the surface fracture width of the wire-sawn silicon wafer, where the fracture width is extracted by an image processing method. A series of silicon wafers are processed and the surface fracture parameters and SSD depth are measured to validate the model. The determined results are compared with the experimental ones. This research is expected to evaluate the SSDs in the silicon wafer quickly and accurately.

2. SSD depth model

2.1. SSD depth vs surface fracture parameters

In diamond wire sawing, a series of abrasive grits on the saw wire scratch the workpiece, and most of them have an irregular shape. The abrasive grit can be divided into two parts. One part is covered with an electroplated layer, and the other part is the protrusion which takes part in the material removal. In the actual wire sawing, the penetration depth of an abrasive grit is usually a few tenths of a micrometer, which is much smaller than the protrusion size of several micrometers (about 1/2 to 2/3 of the grit diameter). Due to the size difference, most researchers simplify the protrusion tip as a cone. Fig. 1(a) shows a scratch groove on a brittle material generated by a conical indenter, which is used to simulate the generation of scratch grooves on

the wafer surface. Scratching can be regarded as a series of indentations along the scratch direction. Fig. 1(b) shows an indentation-induced median-lateral crack system in the brittle material. The material above the lateral crack (yellow region) is removed when the lateral crack propagates outward and to the workpiece surface. This results in the formation of brittle fractures, such as fractured grooves and pits, on the workpiece surface. The fracture depth and width can be estimated by the lateral crack size. The median crack remains in the workpiece thereby generating SSDs. As a result, the SSD depth can be equivalent to the median crack length. The fracture depth c_{li} and SSD depth SSD_{i} can be respectively given by [10]:

$$c_{\mathrm{li}} \propto F_{\mathrm{ni}}^{1/2} \tag{1}$$

$$SSD_{\mathrm{i}} = c_{\mathrm{mi}} \cos\varphi_{\mathrm{i}} \propto F_{\mathrm{ni}}^{2/3} \times \cos\varphi_{\mathrm{i}} \tag{2}$$

where F_{ni} is the normal load; c_{mi} is the median crack length; φ_{i} is the inclination angle of the median crack [11]; i represents the parameters for the ith-related fracture.

The relationship between the fracture depth c_{li} and width c_{wi} can be expressed as [8]:

$$\frac{c_{\mathrm{wi}}}{c_{\mathrm{li}}} \propto F_{\mathrm{ni}}^{1/8} \tag{3}$$

Compared Eq. (1) to Eq. (3), it can be obtained:

$$c_{\mathrm{li}} = \alpha c_{\mathrm{wi}}^{4/5} \tag{4}$$

$$SSD_{\mathrm{i}} = \beta c_{\mathrm{wi}}^{16/15} \tag{5}$$

where α and β are two correction factors that depend on the indenter geometries, workpiece material properties, coolant performance, machine tool vibration, etc. The values of α and β can be fitted out by experiments. Eq. (4) and Eq. (5) indicate that c_{li} and SSD_{i} can be determined by c_{wi}.

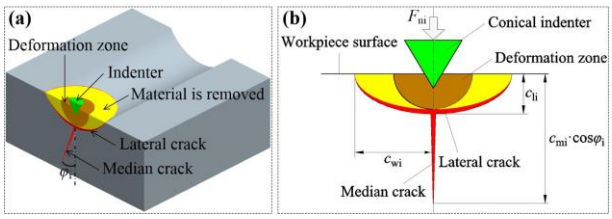

Figure 1. (a) A scratch groove on a brittle material generated by a conical indenter; (b) an indentation-induced median-lateral crack system in the brittle material.

2.2. Digital extraction of surface fracture parameters

Fig. 2(a) shows a micrograph image of the wafer surface. To quickly extract the fracture parameters, an image processing method is presented and achieved by using MATLAB. Firstly, the micrograph image is converted into a gray-scale image (Fig. 2(b)) and a binary image (Fig. 2(c)) to reduce the computation. Secondly, the erosion-reconstruction process is utilized to remove the image noises which includes erosion and dilation operation. The erosion operation can be expressed as:

$$\mathbf{E} = (\mathbf{I}_{\mathrm{e}} \otimes \mathbf{B}_1) = \{ j : \mathbf{B}_1(j) \subseteq \mathbf{E} \} \tag{6}$$

where $\mathbf{E}$ is the matrix of the erosion image; $\mathbf{I}_{\mathrm{e}}$ is the matrix of the input image; $\mathbf{B}_1$ is a shrinkage matrix; j is a certain element in matrix $\mathbf{I}_{\mathrm{e}}$; the operator $\otimes$ denotes an erosion operation. The dilation operation is conducted on the erosion image repeatedly until the pixel values of the erosion image are no longer changed, which can be expressed as:

$$\mathbf{P}_{q+1} = \{ j : (\mathbf{P}_q \oplus \mathbf{B}_2) \cap \mathbf{E} \} \tag{7}$$

$$\mathbf{P}_q \oplus \mathbf{B}_2 = \{ j : (\tilde{\mathbf{B}}_2(j) \cap \mathbf{P}_q) \subseteq \mathbf{P}_q \} \tag{8}$$

where $\mathbf{P}_q$ is the matrix of the reconstruction image after the qth iteration (q = 1, 2, 3…); $\mathbf{B}_2$ is the expansion matrix; $\tilde{\mathbf{B}}_2$ is the reflection of $\mathbf{B}_2$; and operator $\oplus$ denotes the dilation operation. The number of connected domains in the image is reduced after the erosion-reconstruction process, as shown in Fig. 2(d). Finally, each connected domain is framed by a rectangle which is regarded as a brittle fracture, as shown in Fig. 2(e). The fracture width c_{wi} can be determined by extracting the rectangle size, and then the fracture depth c_{li} and SSD depth SSD_{i} can be determined according to Eq. (1) to Eq. (5).

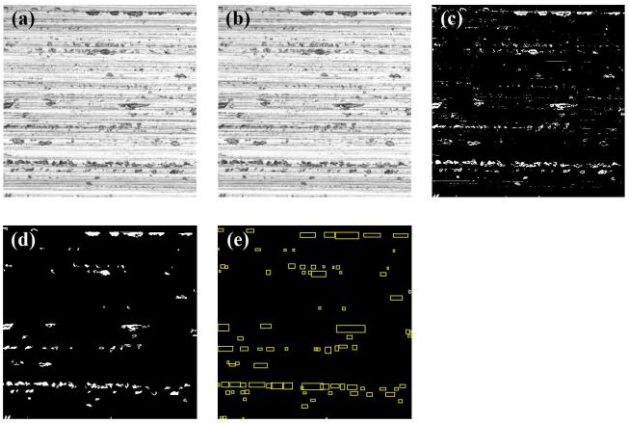

Figure 2. (a) original image; (b) gray-scale image; (c) binary image; (d) erosion-reconstruction image; (e) image with the framed.

3. Experimental

To validate the SSD model, a series of experiments were conducted on (100) single-crystal silicon ingots using multi-wire sawing equipment (QPJ1665, Dalian Linton NC Machine Co., Ltd), as shown in Fig. 3(a). Table 1 shows the silicon ingot's material properties and the saw wire's parameters. The silicon ingot was sliced into many silicon wafers with a size of 156 mm × 156 mm × 0.2 mm (Fig. 3(b)). Three different silicon wafers (No. 1, 2, and 3) were obtained under the feed rates of 0.5, 1.5, and 2.5 mm/min and the wire speed of 1500 m/min. Five small samples were cut from the center of each silicon wafer since the center has stable machined quality. The size of each sample is about 10 mm × 10 mm and the interval between two adjacent samples is about 10 mm (Fig. 3(b)). The sample's surface micrograph was obtained by laser scanning confocal microscopy (OLS4000, Olympus Corporation), and its subsurface micrograph was obtained with cross-section scanning microscopy.

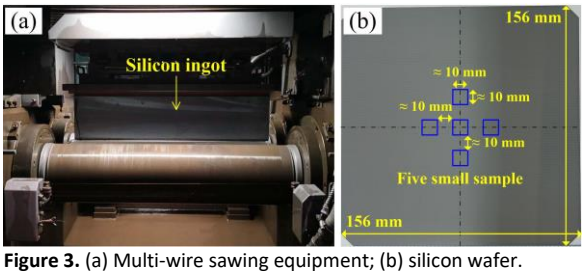

Figure 3. (a) Multi-wire sawing equipment; (b) silicon wafer.

Table 1 Silicon ingot's material properties and saw wire's parameters.

Silicon ingot		Saw wire	
Density	2.33 g/cm^3	Abrasive diameter	12.0 μm
Young's modulus	129.5 GPa	Wire diameter	86.9 μm
Poisson's ratio	0.24	Core diameter	74.4 μm
Hardness	9.5 GPa	Protrusion height	5.4 μm
Fracture toughness	0.93 MPa · $\sqrt{\text{m}}$	Abrasive density	424 grits/mm^2

4. Results and discussions

Fig. 4(a) and Fig. 4(b) show the surface and subsurface micrograph images of a representative sample from silicon wafer 3 (feed rate is 2.5 mm/min), respectively. It can be found from Fig. 4(a) that there are many ductile grooves and brittle fractures on the wafer surface, indicating that the material is removed in both ductile and brittle modes in diamond wire sawing of silicon ingot [12]. The brittle fractures are characterized by fractured grooves and pits. For each surface micrograph image, a profile perpendicular to the scratch grooves and across the largest fracture (selected by the naked eye) is obtained. According to the profile, the width c_{wm} and depth c_{lm} for the largest fracture are measured, and their values are 8.6 μm and 1.3 μm, respectively. The maximum subsurface crack depth in each subsurface micrograph image was regarded as the SSD depth. Fig. 4(b) shows two subsurface median cracks, and their induced SSD depth $SSD_{\text{m}} = \max(SSD_1, SSD_2) = 4.7\ \mu\text{m}$. Also, the lateral crack profile is shown, the material above which has been removed resulting in a brittle fracture on the wafer surface.

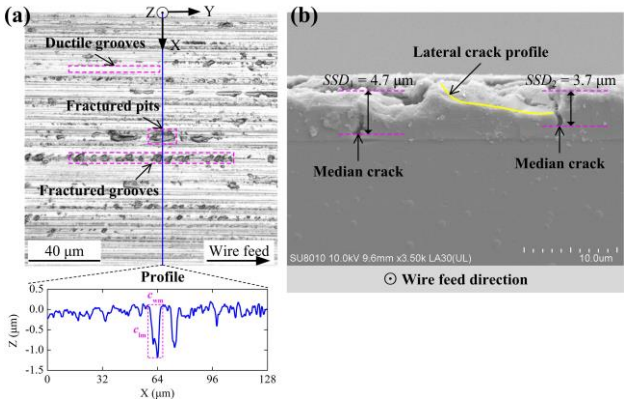

Figure 4. (a) Surface and (b) subsurface micrograph images of a representative sample from silicon wafer 3.

Five surface and subsurface micrograph images are obtained from five samples of each silicon wafer, and the values of c_{wm}, c_{lm}, and SSD_{m} are measured. The measured and determined (with the image-processing-based model) values are compared, and their relative error is defined as:

$$error = \frac{|\text{Measured value} - \text{Determined value}|}{\text{Measured value}} \times 100\% \quad (9)$$

Fig. 5(a) shows the measured values of c_{wm} are almost equal to those determined ones for all fifteen surface micrographs, with an average relative error of 5.4%. Fig. 5(b) shows the measured values of c_{wm} and c_{lm} for all fifteen surface micrographs distributing along the curve of $c_{\text{lm}} = 0.298 \times c_{\text{wm}}^{4/5}$, verifying the reasonability of Eq. (4). The average value of five c_{wm} (c_{w}) and that of five SSD_{m} (SSD) for each silicon wafer are used to determine the value of $\beta = 0.595$, as shown in Fig. 5(c), thus validating the reasonability of Eq. (5). Furthermore, the values of SSD are determined with the values of c_{w} which are compared with those measured ones, as shown in Fig. 5(d). The determined values agree well with the measured ones with an average relative error of 11.7%. Fig. 5(a) to Fig. 5(d) show the accuracy of the image processing method and SSD depth model. When a laptop is used (Processor: Intel Core i7-8550U 1.8GHz, installed memory: 16.0 GB), the total time for the extraction of fracture parameters and the determination of SSD depth is less than 15 seconds for each image, indicating the method is quick.

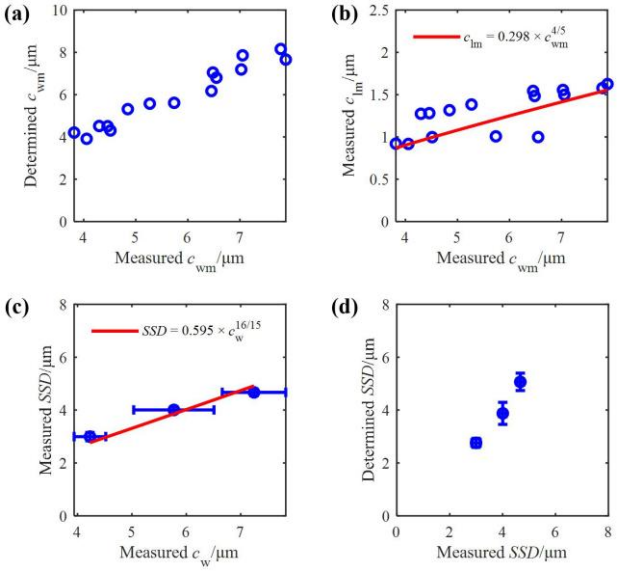

Figure 5. (a) Comparison between the measured and determined values of c_{wm}; (b) Relationship between the measured values of c_{wm} and c_{lm}; (c) Relationship between the measured values of c_{w} and SSD; (d) Comparison between the measured and determined values of SSD.

5. Conclusions

Based on the scratch fracture mechanics of brittle materials, this paper models the SSD depth with the surface fracture parameters for the diamond wire sawing of silicon wafers, where the fracture parameters are extracted with a proposed image processing method. The SSD depth model is validated experimentally. The image processing method can be used to accurately extract the fracture width with an extraction error of 5.4%. Within about 15 seconds, the model can be utilized to accurately determine the SSD depth with an average relative error of 11.7%. It provides an important means for non-invasive evaluation of the SSDs in diamond wire sawing of silicon wafer. In the future, it is expected that the model will be extended to on-line inspection of the SSDs in wire-sawing of silicon wafers.

Acknowledgement

The authors would like to express thanks to the Innovation and Technology Commission (ITC) of the Government of the Hong Kong Special Administrative Region, China (GHP/142/19SZ), the research studentships from the Research Committee of The Hong Kong Polytechnic University (RH5Q).

References

[1] Ge M, Zhang C, Wang P, Li Z and Ge P 2023 Modeling of electroplated diamond wire and its application towards precision slicing of semiconductors *J. Manuf. Process* **87** 141-49.

[2] Ge M, Chen Z, Wang P and Ge P 2022 Crack damage control for diamond wire sawing of silicon: The selection of processing parameters *Mater. Sci. Semicon. Proc.* **148** 106838.

[3] Costa E C, Xavier F A, Knoblauch R, Binder C and Weingaertner W L 2020 Effect of cutting parameters on surface integrity of monocrystalline silicon sawn with an endless diamond wire saw *Sol. Energy* **207** 640-50.

[4] Teomete E 2013 Wire saw process-induced surface damage characterization *Arab. J. Sci. Eng.* **38** 1209-15.

[5] Suzuki T, Nishino Y and Yan J 2017 Mechanisms of material removal and subsurface damage in fixed-abrasive diamond wire slicing of single-crystalline silicon *Precis. Eng.* **50** 32-43.

[6] Kumar A, Kaminski S, Melkote S N and Arcona C 2016 Effect of wear of diamond wire on surface morphology, roughness and subsurface damage of silicon wafers *Wear* **364-365** 163-68.

[7] Liu T, Ge P, Bi W and Gao Y 2017 Subsurface crack damage in silicon wafers induced by resin bonded diamond wire sawing *Mater. Sci. Semicon. Proc.* **57** 147-56.

[8] Xiao H, Wang H, Yu N, Liang R, Tong Z, Chen Z and Wang J 2019 Evaluation of fixed abrasive diamond wire sawing induced subsurface damage of solar silicon wafers *J. Mater. Process Technol.* **273** 116267.

[9] Wang L, Gao Y, Li X, Pu T and Yin Y 2020 Analytical prediction of subsurface microcrack damage depth in diamond wire sawing silicon crystal *Mater. Sci. Semicon. Proc.* **112** 105015.

[10] Xiao H, Yin S, Wang H, Liu Y, Wu H, Liang R and Cao H 2021 Models of grinding-induced surface and subsurface damages in fused silica considering strain rate and micro shape/geometry of abrasive *Ceram. Int.* **47** 24924-41.

[11] Wang L, Gao Y, Pu T and Yin Y 2021 Fracture strength of photovoltaic silicon wafers cut by diamond wire saw based on half-penny crack system *Eng. Fract. Mech.* **251** 107717.

[12] Yin S, Xiao H, Wu H, Wang C and Cheung C F 2022 Image-processing-based model for the characterization of surface roughness and subsurface damage of silicon wafer in diamond wire sawing *Precis. Eng.* **77** 263-74.